Article

Vegetation Impact and Recovery from Oil-Induced Stress on Three Ecologically Distinct Wetland Sites in the Gulf of Mexico

Kristen Shapiro *, Shruti Khanna and Susan L. Ustin

Department of Land, Air, and Water Resources, University of California, Davis, CA 95616, USA; shrkhanna@ucdavis.edu (S.K.); slustin@ucdavis.edu (S.L.U.)
* Correspondence: kdshapiro@ucdavis.edu; Tel.: +1-510-579-1597

Abstract: April 20, 2010 marked the start of the British Petroleum Deepwater Horizon oil spill, the largest marine oil spill in US history, which contaminated coastal wetland ecosystems across the northern Gulf of Mexico. We used hyperspectral data from 2010 and 2011 to compare the impact of oil contamination and recovery of coastal wetland vegetation across three ecologically diverse sites: Barataria Bay (saltmarsh), East Bird's Foot (intermediate/freshwater marsh), and Chandeleur Islands (mangrove-cordgrass barrier islands). Oil impact was measured by comparing wetland pixels along oiled and oil-free shorelines using various spectral indices. We show that the Chandeleur Islands were the most vulnerable to oiling, Barataria Bay had a small but widespread and significant impact, and East Bird's Foot had negligible impact. A year later, the Chandeleur Islands showed the strongest signs of recovery, Barataria Bay had a moderate recovery, and East Bird's Foot had only a slight increase in vegetation. Our results indicate that the recovery was at least partially related to the magnitude of the impact such that greater recovery occurred at sites that had greater impact.

Keywords: oil spill; marshes; AVIRIS; spectroscopy; remote sensing; oil impact; cordgrass; mangroves; Mississippi Deltaic Plain; Gulf of Mexico

1. Introduction

The British Petroleum Deepwater Horizon (BP-DWH) oil spill was the largest marine oil spill in US history [1]. The spill deposited oil along the shoreline of the Mississippi Deltaic Plain (MDP) which is home to the largest expanse of contiguous wetlands in the United States [2]. Wetlands offer a variety of ecological services including water purification, carbon storage, storm protection and nutrient cycling [3]. The MDP also supports one of the world's largest petroleum development infrastructures and is subject to chronic low-level oil spills [3]. The coastal wetlands and barrier islands of the MDP are already experiencing extreme land loss at the rate of ~43 km^2/year [4]. Oil contamination can escalate the rate of land loss through reduction of vegetation cover and loss of live plant roots which stabilize the soil [5].

The physical effects of oil on plant health are varied and based on a number factors including plant type, oil type, oil concentration, persistence, and extent of oil penetration into the marsh [6]. Plant mortality is higher when oil coats the leaf surfaces leading to reduced gas exchange via the stomata [7]. This results in oxygen-stressed roots (or pneumatophores in the case of mangroves) that further reduce plant growth and water uptake for transpiration resulting in high temperature stress. Plant roots are further stressed when oil coats the soil resulting in reduced soil conditions [7]. These stresses are manifested through leaf chlorosis and stem discoloration as plants lose chlorophyll [8]. Changes in plant health can be measured remotely by looking at the spectral response of vegetation.

Healthy plants reflect strongly in the near-infrared region of solar radiation and absorb strongly in the visible region due to photosynthetic pigments. The sharp increase in leaf reflectance between 680 and 750 nm is called the "red edge". As plants lose pigments due to chlorosis, the red edge becomes less sharp, reflectance in the visible region rises, and reflectance in the near-infrared (NIR) drops [9]. Thus plant chlorosis can be measured using spectral pigment indices such as the Normalized Difference Vegetation Index (NDVI) and modified NDVI (mNDVI) that track changes in chlorophyll content [10,11]. Furthermore, the red edge can be used as an indicator of plant stress based on a shift in its wavelength position and a decline in its slope [8,9].

When plants experience stress, they may also start to lose water, which manifests as a lower absorption in the shortwave-infrared region (1500–2500 nm) [8,12]. Water loss can be measured using spectral indices such as Normalized Difference Infrared Index (NDII), Absorption Depth of Water at 980 nm (ADW1) and ADW at 1240 nm (ADW2) [12,13]. As vegetation senesces, angle indices like Angle at NIR (ANIR) and Angle at Red (ARed) can track landcover change from healthy green vegetation to non-photosynthetic vegetation (NPV) and eventually soil [14].

Remote sensing for monitoring spatially extensive disasters such as the BP-DWH oil spill is important since field surveys are often costly and time consuming, yet may still fail to cover the entire impacted area. Furthermore, sensitive wetland ecosystems that have been stressed by oil contamination can be further damaged by site visits and remediation activities [15,16]. Remote sensing offers an alternative to extensive field surveys by providing 100% sampling of the affected area, as well as repeat monitoring that can extend over multiple years to track recovery in addition to impact. A handful of remote sensing studies have mapped plant stress in response to oil contamination [8,13,17,18]. A popular method for tracking oil-induced stress has been to identify a shift in the red edge towards longer [8,19,20] or shorter wavelengths [21]. However, Khanna *et al*. [22] successfully used pigment and plant water spectral indices to elucidate patterns of oil impact on saltmarsh vegetation in Barataria Bay, Louisiana.

The objective of this study is to compare the impact of the BP-DWH oil spill on wetland vegetation and monitor recovery in the following year across three diverse ecosystems in the MDP. Several studies have documented the impact from the BP spill for the gulf wetlands, but the majority of these studies have focused on a single marsh vegetation species or a single site in the gulf [5,17,23–25]. We wanted to compare the effect of the BP-DWH oil spill across multiple ecosystems in the gulf as well as evaluate recovery of live foliar canopy a year later. We used hyperspectral imagery from the fall of 2010 to assess the impact of oil-induced stress on wetland vegetation and compared it to imagery from 2011 to look for evidence of recovery from the oil. To evaluate oil impacts on the marsh ecosystem, we used several vegetation indices as measures of plant stress. For recovery, we used change detection of classified images between years to see if the area of green vegetation had increased or decreased.

2. Data and Methods

2.1. Study Sites

The MDP estuary complex contains the largest saltmarsh area and the second largest fresh marsh area in the continental United States [26]. The MDP also contains barrier islands that support black mangrove shrublands and serve a protective role for the mainland by absorbing the brunt of tidal surges from incoming storms [27]. Understanding the role of vegetation and its response to a contamination event is important for effective management in the face of continued land loss as well as effective recovery in times of disaster [28]. Hence we chose three sites for our study: Barataria Bay (saltmarsh), East Bird's Foot (freshwater and intermediate marsh), and the Chandeleur Islands (mangrove-cordgrass marshland) that represent three distinct ecosystems of the MDP (Figure 1).
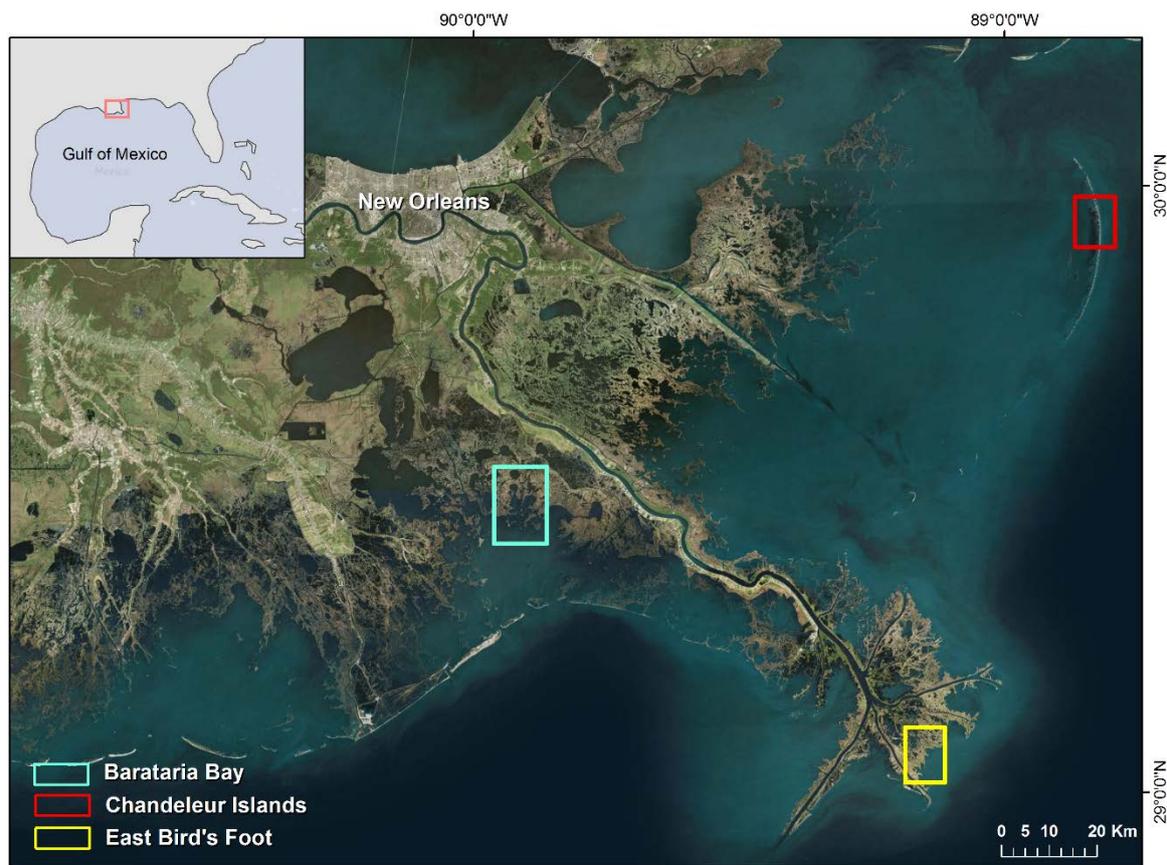
Figure 1. Location of all three study sites in the Gulf of Mexico.

Barataria Bay (BB) is located approximately 160 km from the spill site in an interlobe basin between the current Bird's Foot delta and the abandoned Lafourche delta lobes [29]. BB consists solely of saltmarshes as it no longer receives significant fresh water or sediment input due to the levees along the Mississippi River and the closure of Bayou Lafourche. The dominant vegetation in the low intertidal saltmarshes is *Spartina alterniflora* (saltmarsh cordgrass) and *Juncus roemerianus* (needlegrass rush), with subdominants *Spartina patens* (salt meadow cordgrass), *Distichlis spicata* (saltgrass) and *Batis maritima* (saltwort) more common in the higher marsh [3]. Since the BP-DWH oil spill occurred offshore, the oil came in with the tides and primarily contaminated the seaward edges of these marshes. Our field data sources (Section 2.2) indicate that the marsh edge vegetation in BB is dominated by *S. alterniflora* followed by *J. roemerianus*.

Our second study site is on the Chandeleur Islands (CI), a 72 km long barrier island chain located approximately 140 km from the spill site. The islands form a diverse landscape of beaches, dunes, and marshes. The Chandeleur Islands are frequently overwashed due to tidal surges during tropical and temperate storms. As a result, the vegetation plays an important role in stabilization and sand deposition [27]. CI is a remote area and studies in this area are rare, even in the aftermath of the BP-DWH spill. However, based on the Natural Resource Damage Assessment (NRDA) data [30], our field data, and high resolution aerial imagery (AeroMetric), we determined that our study area is dominated by *Avicennia germinans* (black mangrove) and *Spartina alterniflora* with subdominants *Salicornia* spp. (pickleweed) and *Distichlis spicata* (seashore saltgrass).

The East Bird's Foot (EBF) site is located in the current primary delta lobe approximately 80 km from the spill site. This area continues to receive fresh water and sediment from the Mississippi River, and contains approximately 61,650 acres of wetlands, 81% of which are fresh water, 17% are intermediate, and 2% are brackish or saline [31]. The dominant vegetation for intermediate marshes

is *Spartina patens*, *Phragmites australis* (common reed), *Sagittaria falcata* (bull-tongue arrowhead), and *Alternanthera philoxeroides* (alligator weed) [3,32]. The dominant vegetation in freshwater marshes is *Panicum hemitomon* (maiden cane), *Sagittaria falcata*, *Eleoharis* spp. (spike rush), and *Alternanthera philoxeroides* [3,32]. The area of EBF most affected by oil and present in our image data was almost exclusively dominated by *Phragmites australis* [32–34].

2.2. Field Data

For the selection of oiled and oil-free areas at each site, we used shoreline data collected from May through September of 2010 provided by the Shoreline Cleanup Assessment Technique (SCAT) program through the Environmental Response Management Application (ERMA), part of the National Oceanic and Atmospheric Administration (NOAA). The SCAT data is a collection of multiple ground surveys starting from May 2010 which contain mapped shorelines based on observed presence of oil. The shorelines are assigned a level of oil contamination based on four broad descriptive categories: Heavy, Moderate, Light, and No Oil [33].

For information on plant species affected by oil, we also relied on field data collected by David Baker of Tulane University in all three study areas between 2012 and 2014 as part of this study. 10 m × 10 m plots were collected along 100 m transects that started at the water's edge and moved inland perpendicularly to the shore. Approximately eight points were collected per transect spread evenly along its length with 46 transects collected. Species composition, cover, and degree of oiling were noted for each plot. This data was further supplemented with vegetation composition data from the Coastwide Reference Monitoring System (CRMS) [32,35] and the Natural Resource Damage Assessment (NRDA) [30].

2.3. Image Data and Preprocessing

To test the impact of oil on the wetlands in 2010, we used AVIRIS imagery from September (for BB and CI) and October (for EBF) of 2010 (Table 1). According to NOAA tide tables (http://tidesandcurrents.noaa.gov/), tide levels were only different between imagery collection dates for Chandeleur Islands (Table 1). This was taken into account when interpreting the results for Chandeleur Islands.

Table 1. Site information regarding data acquisition for each study site (East Bird's Foot—EBF, Barataria Bay—BB, and Chandeleur Islands—CI) such as time and date of acquisition, pixel resolution, number of flightlines, and tidal stage. Water levels are calculated based on the mean lower low water (MLLW) height datum.

Site	Year	Flight Dates	Pixel Resolution (m)	# Flightlines	Water Level (m)	Shoreline Analyzed (km)
BB	2010	09/14	3.5 × 3.5	4	0.21	30.4
	2011	08/25	7.7 × 7.7	2	0.25	
CI	2010	09/21	3.4 × 3.4	2	0.66	3.2
	2011	08/11	7.7 × 7.7	2	0.25	
EBF	2010	10/03	3.4 × 3.4	2	0.11	4.3
	2011	10/14	3.4 × 3.4	2	0.18	

To test recovery in 2011, a year after the oil spill ended, we acquired AVIRIS data over the same sites in August 2011 (For BB and CI) and in October 2011 (for EBF). While the imagery for BB and CI was flown a month earlier in 2011, these date differences are not likely to affect the results as the growing conditions were similar for the months in which the data was collected. In 2010 and 2011, both sites received substantial rainfall the month preceding the imagery and very little rainfall in the month when the imagery was acquired. The average temperature for both sites ranged from 27–31 °C during September 2010 and August 2011. Both the 2010 and 2011 data were atmospherically calibrated,

georectified, co-registered [13] and resampled to the 2011 spatial resolution (7.7 m for BB and CI and 3.4 m for EBF). We calculated spectral indices (Table 2) for each site in 2010.

Table 2. Seven indices chosen to study severity of oil impact. R_R, R_{NIR} and R_{SWIR} are the reflectance values in the Red, Near-Infrared (NIR), and Shortwave-Infrared (SWIR) bands, respectively, and λ_R, λ_{NIR}, and λ_{SWIR} are the center wavelengths for the Red, NIR and SWIR bands.

Acronym	Formula	Plant	References
NDVI	$(R_{NIR} - R_R)/(R_{NIR} + R_R)$	chlorophyll content and/or leaf area of the plant	[11]
mNDVI	$(R_{750} - R_{700})/(R_{750} + R_{700})$	chlorophyll content and/or leaf area of the plant	[10]
NDII	$(R_{NIR} - R_{923})/(R_{NIR} + R_{923})$	Water content	[12]
ANIR	Angle between (R_R, λ_R), (R_{NIR}, λ_{NIR}), and $(R_{SWIR}, \lambda_{SWIR})$	Phenology and stress	[14,36]
ARed	Angle between (R_R, λ_R), (R_R, λ_R), and (R_{NIR}, λ_{NIR})	Phenology and stress	[13,36]
ADW1	$0.5 \times (R_{1070} + R_{890}) - R_{990}$	Water content	[13]
ADW2	$0.5 \times (R_{1270} + R_{1070}) - R_{1167}$	Water content	[13]

Although we had access to high spatial resolution aerial imagery, QuickBird imagery, and WorldView-2 imagery for some of these sites, we chose the AVIRIS imagery for our comparative analysis because the spectral range (350–2500 nm) and spectral resolution (5–10 nm bandwidth) required to calculate our suite of indices were not available with any other imagery.

We also classified the AVIRIS images from both years into five classes: water, green vegetation, NPV, soil, and submerged aquatic vegetation (SAV) using a decision tree classifier [13]. The NPV class contains dead, dying, and senescent vegetation. We combined the NPV and soil classes into one combined NPV-Soil group for the analysis. The decision tree method applied in this study uses indices to differentiate classes that take advantage of their biophysiological differences [22,37]. The index thresholds that provided maximum differentiation between classes were selected based on ANOVA tests and then used to build a binary decision tree. The decision tree method uses inputs derived from multiple binary nodes that are based on the characteristics of the dataset. The user builds the decision tree and chooses the threshold values that are used at each node in the tree. At each node, the classifier splits the data into one of two possible classes or groups. This method is analogous to using a plant identification key, such as the Jepson Manual of Higher Plants of California [38].

2.4. Image Analysis

2.4.1. Selection of Oiled and Oil-Free Shores

Oil first appeared on the shores of EBF and CI in the last week of April and first week of May 2010 [39,40]. However, we were unable to directly map the presence of oil on the marsh surface in the images acquired over EBF and CI in September–October. Two factors may have impacted our ability to map oil on the surface. Firstly, oil might have been present under the plant canopy obstructing its spectral signal. Secondly, plant water absorption features in the spectrum overlap with oil absorptions, making it difficult to detect oil even if it is on the surface of the plants.

On the other hand, oil reached the shores of BB in mid-July, and continued to arrive through August–September [41–44]. During the time the imagery was acquired, it was still fresh and coated the soil surface (Khanna, personal observation). Therefore, we were able to accurately classify oiled soil and NPV pixels for the September 19, 2010 image data (overall accuracy: 95%, Kappa: 0.88, *n* = 40) [13].

Since we were only able to map actual oil contamination at the BB site, we used the publically available SCAT data of oiled shorelines, recorded by visual observation during the period of the oil spill. We compared SCAT-observed shorelines to our classified oiled pixels in BB (Figure 2). We found

that, of the three levels of oiling in the SCAT database for BB, the "Moderate" and "Light" oiled shorelines did not consistently correspond to regions of oiled pixels in our BB imagery. Figure 2c,d show examples of moderately oiled and lightly oiled shorelines. Moderately oiled shorelines had fragmented sections of oiled pixels, and lightly oiled shorelines had very few oiled pixels. We limited our analysis to "Heavily" oiled shorelines, comparing them to oil-free shorelines at all three sites, because the presence of oil-free regions within "Moderate" and "Light" oiled SCAT shorelines would weaken the spectral signal of the oil impacts (making it harder to detect). Shorelines selected for analysis in BB, CI and EBF are shown in Figures 2–4.
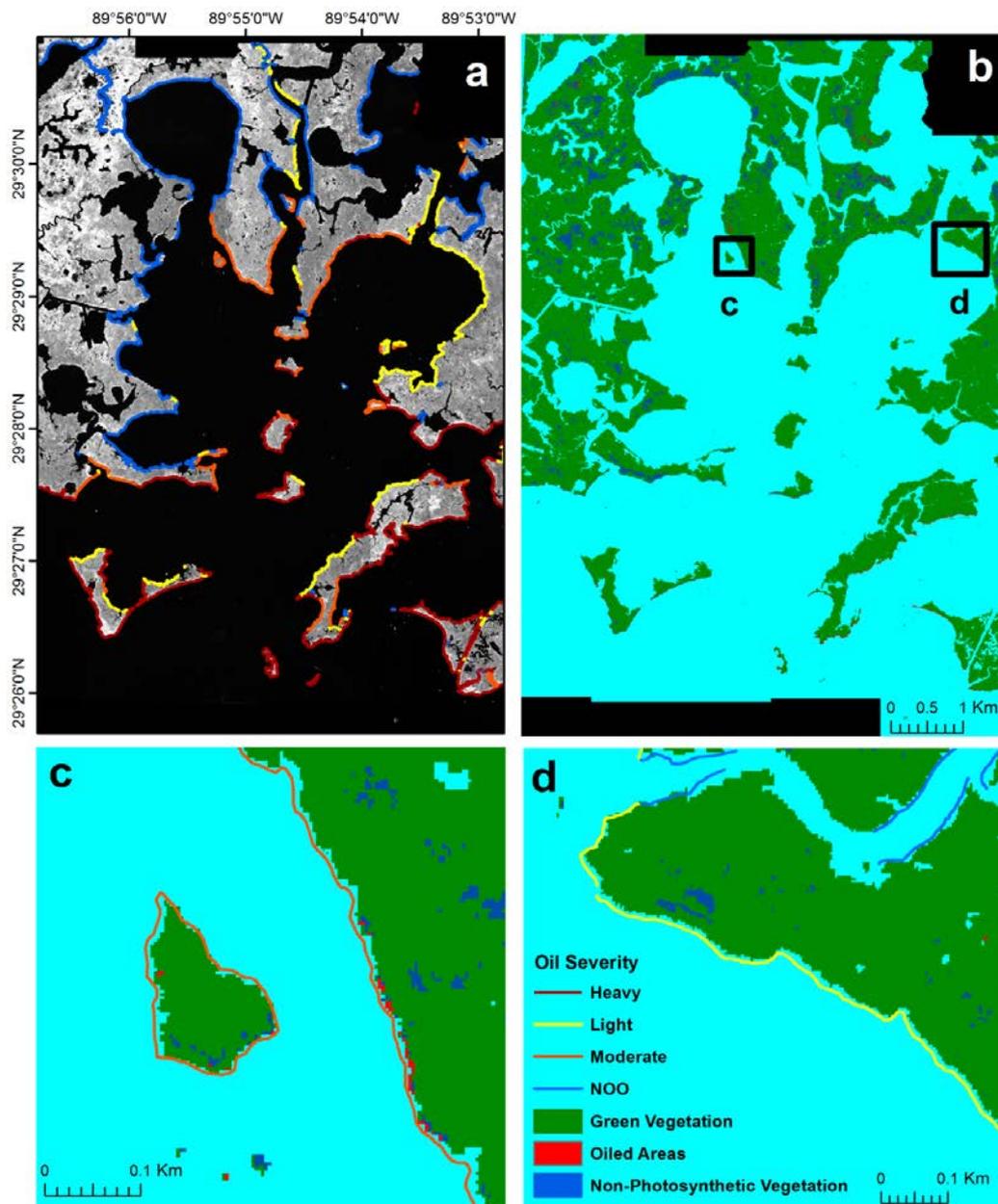

Figure 2. (**a**) SCAT oiled shoreline data overlaid on the AVIRIS flightlines acquired September 14, 2010 over Barataria Bay, (**b**) landcover classification showing location of inset c and d, (**c**) a shoreline designated as moderately oiled by SCAT, with patches of oiled pixels, and (**d**) a shoreline designated as lightly oiled by SCAT with very few oiled pixels.
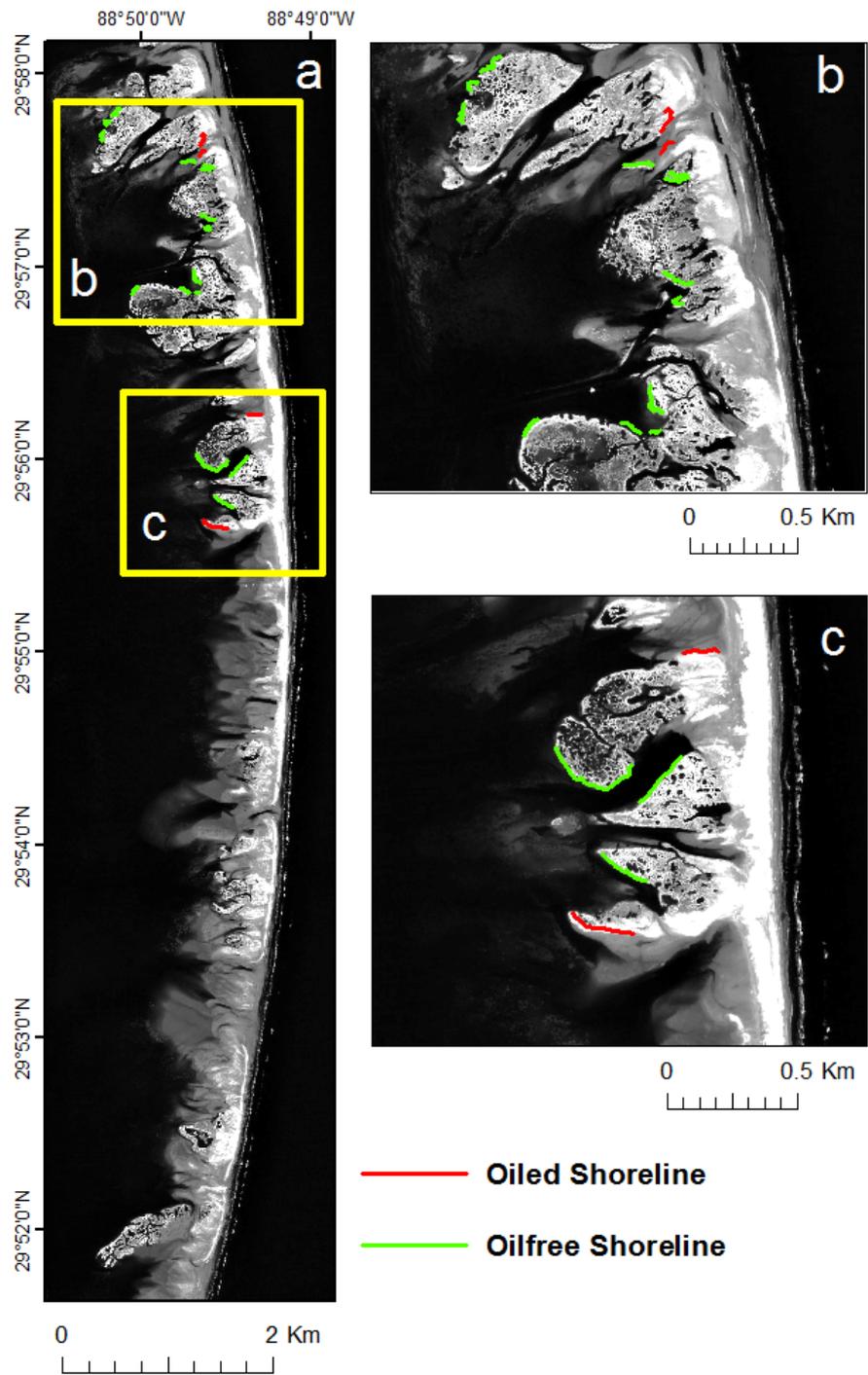
Figure 3. (**a**) SCAT oiled and oil-free shoreline data selected for analysis overlaid on the AVIRIS flightlines acquired over Chandeleur Islands on September 21, 2010 with detailed views of two sections, (**b**) and (**c**) affected by oiling.
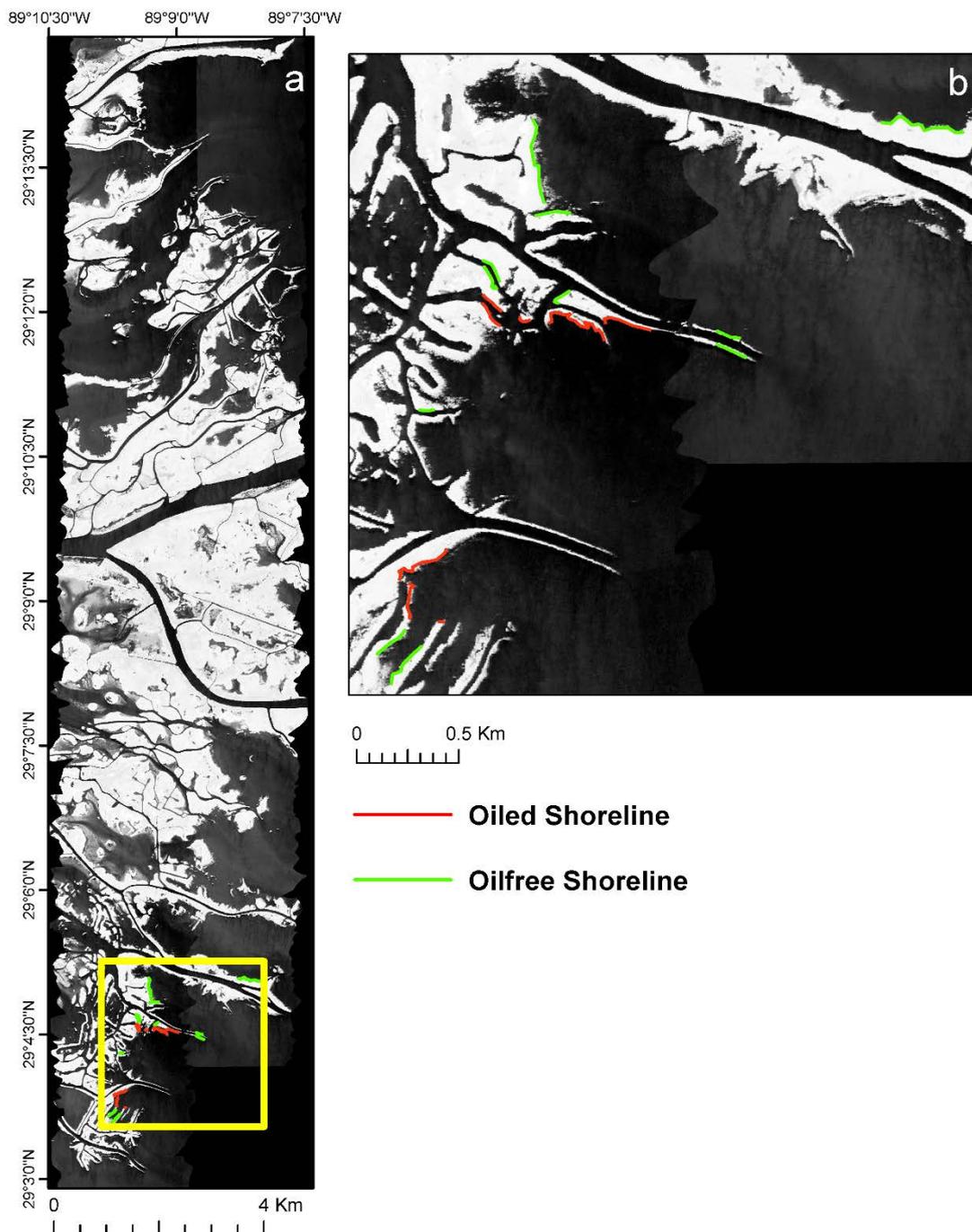
Figure 4. (**a**) SCAT oiled and oil-free shoreline data overlaid on the AVIRIS flightlines acquired October 3, 2010 over East Bird's Foot with (**b**) detailed view of the most affected section.

Once the shorelines to be analyzed were selected, we overlaid the oiled and oil-free shoreline vectors on the index and classification images, and created a 16 m buffer inland from the shorelines. There were two reasons for this: (1) Khanna *et al*. [13] showed that in BB, oil impacts were significant within the first 16 m perpendicular to the shoreline, and (2) the bathymetry and tidal interaction in each site creates very different patterns of oiling. In BB, shallow bathymetry and the tide create different oil residence times and penetration distances, leading to differential impacts moving inland from the shore [28]. In CI, the vegetation grows on low-lying dunes on the landward side, where ocean waves are able to penetrate far across the islands. The frequent tidal overwashing could have dispersed the oil

across the island, potentially causing similar oil impacts irrespective of the distance of the vegetation from the shoreline [27]. In EBF, the hydrology has been greatly modified by human activity, making it the most fragmented and developed area of all three sites. Given these differences, we identified an impact buffer for each site. The 16 m buffer translates to a 2-pixel buffer for images with 7.7 m pixels and a 5-pixel buffer for the images with 3.4 to 3.5 m pixels.

2.4.2. Comparison of Oil Impact across Sites

For the analysis of oil impact, we focused on seven spectral indices (Table 2) from different wavelength regions of the solar spectrum, ranging from the visible through the shortwave-infrared that track changes in chlorophyll content and/or leaf area of the plant (Normalized Difference Vegetation Index: NDVI and modified NDVI: mNDVI), changes in plant condition: green, senescent, dead (Angle at NIR: ANIR and Angle at Red: ARed), and changes in plant water content (Normalized Difference Infrared Index: NDII, Water Absorption at 980 nm: ADW1, and Water Absorption at 1240 nm: ADW2) (Table 2). We tested these multiple indices against the predictor variable of oiling. No single index is optimal for all conditions; plant stress can be expressed as pigment loss, water loss, leaf area loss, or all three. Consistent responses across these diverse indices indicates the analysis is more robust. Many of these indices are correlated (e.g., ANIR and ARed have two bands in common); however, since they are response variables, there is no requirement that they should be statistically independent. The differences between them highlight how different biophysiological characteristics of the wetland plant communities respond to oil-induced stress.

The red edge inflection point (REIP) [9] has been useful in detecting stress and senescence and has been used to detect stress from oil [8], but was not used in this study. Previous work in the response to the BP-DWH oil spill in Barataria Bay showed much of the intertidal vegetation was coated with oil and was dead and partially removed by tidal action at the time the imagery was acquired [13]. Thus many pixels affected by oil no longer had green foliage and the spectral response lacked the red edge feature.

We tested for significant differences between index values extracted from oiled and oil-free buffer zones at all three sites using the Mann-Whitney Test—a non-parametric test [45] (Table 3). We could not use a simple *t*-test because our index histograms were either bi-modal or skewed and violated the assumption of normality. We believe both these distributions were due to the mix of landcover types in our data. For many indices (e.g., ANIR, ARed, ADW, mNDVI), soil-NPV and green vegetation had distinct peaks resulting in a bi-modal distribution while some indices like NDVI or NDII exhibited a skewed distribution.

We also calculated Cliff's delta, a measure of effect size for non-normal data [46–48]. Cliff's delta measures the degree of overlap between two populations. It ranges from −1 to +1, where an effect size of 1 or −1 indicates no overlap in the two populations and a value of 0 means the distributions are identical. When interpreting delta, 0.147 represents a small effect (percent of non-overlap is 14.7%), 0.33 represents a medium effect (percent of non-overlap is 33%), and 0.474 represents a large effect (percent of non-overlap is 47.4%) [48]. Unlike significance tests, effect size provides a statistic that is independent of sample size and range of index values. It allowed us to standardize the difference between two populations across many variables (e.g., multiple indices) and to quantify the magnitude of a difference in effect across sites. By using effect sizes, we were able to compare the performance of different indices and their sensitivity to differences in impact across sites.

Table 3. Median values for each index for oil and oil-free shorelines, the U statistic and *p*-values from the Mann-Whitney Test and the effect size as calculated with Cliff's delta. *n* indicates total number of pixels in each study site for all oiled shorelines and oil-free shorelines.

Site	Median		U	*p*-Value	Cliff's Delta
	Oiled	Oil-Free			
BB	*n* = 36,588	*n* = 23,319			
NDVI	0.61	0.68	366,505,856	<0.0001	0.14
mNDVI	0.30	0.37	365,362,851	<0.0001	0.14
NDII	0.20	0.24	361,584,380	<0.0001	0.15
ANIR	0.95	0.50	513,898,843	<0.0001	0.20
ARed	4.67	4.99	348,463,947	<0.0001	0.18
ADW1	219.62	270.51	353,379,597	<0.0001	0.17
ADW2	414.13	484.95	352,463,292	<0.0001	0.17
CI	*n* = 3,089	*n* = 8,460			
NDVI	0.31	0.55	4,782,283	<0.0001	0.63
mNDVI	0.11	0.28	5,436,240	<0.0001	0.58
NDII	0.10	0.36	3,023,503	<0.0001	0.77
ANIR	1.56	0.70	20,080,843	<0.0001	0.54
ARed	4.71	5.56	4,765,186	<0.0001	0.64
ADW1	249.26	425.32	7,584,217	<0.0001	0.42
ADW2	374.55	621.53	7,011,257	<0.0001	0.46
EBF	*n* = 1,620	*n* = 2,982			
NDVI	3.5	0.81	2,822,096	<0.0001	0.17
mNDVI	0.68	0.68	2,663,718	<0.0001	0.10
NDII	0.63	0.63	2,428,518	0.7600	-
ANIR	0.23	0.22	2,122,563	<0.0001	0.12
ARed	5.98	5.98	2,592,410	0.0007	0.07
ADW1	438.40	510.04	2,905,034	<0.0001	0.20
ADW2	478.29	543.92	2,839,563	<0.0001	0.18

2.4.3. Comparison of Recovery from the Oil Spill across Sites

For the analysis of recovery from oil impact, we used the classified images for both years and compared them after classification. We resized the 2010 imagery to the same resolution as the 2011 imagery and overlaid the 16 m buffer used in the oil impact analysis to perform a change detection analysis. Additionally, we included the equivalent buffer distance on the seaward side (mostly water) to take into account any new growth extending outward from the shoreline after 2010. To estimate recovery we looked at total percentage of green vegetation at a site in 2010 and 2011 and any change in area covered by vegetation.

$$PCveg_{2010} = PXveg_{2010}/PXtotal_{2010}$$

where,

$PCveg_{2010}$ = percentage of green vegetation pixels in 2010
$PXveg_{2010}$ = total number of pixels of green vegetation in 2010
$PXtotal_{2010}$ = total number of pixels analyzed

Similarly,

$$PCveg_{2011} = PXveg_{2011}/PXtotal_{2011}$$

The difference between $PCveg_{2010}$ and $PCveg_{2011}$ serves as an indicator of recovery or lack thereof. This analysis was restricted to the oiled shorelines to determine if they recovered.

We tested for significant conversion from the NPV-Soil, and water classes to green vegetation and *vice versa*. Even sub-pixel level misregistration between images from different dates can lead

to overestimation of change by inflating the change from one class to another [49,50]. For example, from 2010 to 2011, some areas converted from water and NPV-Soil to green vegetation and some green vegetation became water or NPV-Soil. We tested whether this exchange between classes was more than expected through random chance using McNemar's Test. This test is used for data that is not independent and examines two proportions for significant differences [51]. It is sometimes referred to as a "within-subjects chi-squared test" and the test statistic (χ^2) is a chi-squared value compared against the critical value to find significance. This test requires a 2×2 contingency table, thus we combined the NPV-Soil and water classes into one class called "other." The results from this test indicate whether the amount of recovery (*i.e.*, conversion of NPV-Soil/Water in 2010 to green vegetation in 2011) was significantly different from any conversion of vegetation with green foliage in 2010 to NPV-Soil/water in 2011.

3. Results

3.1. Comparison of Oil Impact across Sites

The Chandeleur Islands had the highest average Cliff's delta effect size at 0.58, which indicates large differences in vegetation health between the oiled and oil-free shorelines. Barataria Bay had an average effect size of 0.17, which is interpreted to be a small difference between populations. East Bird's Foot had an average effect size of 0.14 which indicates the difference in vegetation condition between the oil and oil-free shorelines was negligible. Across the three sites, the effect size illustrates that CI experienced much more damage in terms of plant health than the other two sites. Table 3 summarizes the results of the Mann-Whitney test and Cliff's delta for the seven spectral indices across the three sites.

Overall, no one index or group of indices (indicators of pigment, water content, or plant condition) were best at measuring oil impact across all three sites; even within index groups (e.g., leaf water content indices), the response was not uniform. Nonetheless, the indices consistently differed between oiled and unoiled pixels and gave similar values of Cliff's delta within sites and prominent differences between sites (Figure 5).
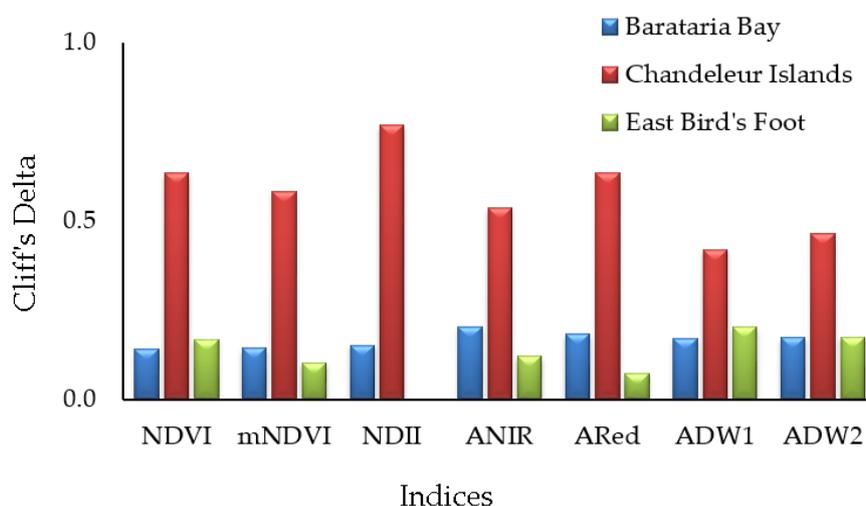

Figure 5. The difference in effect size (Cliff's delta) between the three sites for seven spectral indices.

3.2. Comparison of Recovery from Oil across Sites

For BB, we saw an increase in the percentage of green vegetation, from 34.6% to 48.1%, as the marsh recovered between 2010 to 2011 (Table 4). In CI, there was a large increase in the total percentage

of green vegetation, from 30.9% in 2010 to 65.1% in 2011. In EBF, the change in green vegetation was minimal in the impacted zone (Table 4).

Table 4. Change in total classified area from 2010 to 2011 for each study site. Area of each class is in m^2 (each pixel = 59.3 m^2 for Barataria Bay and Chandeleur Islands and 11.56 m^2 for East Bird's Foot). PCveg is the overall percentage of green vegetation from 2010 to 2011 for each study site along the oiled shorelines. As the buffer zone includes both the landward side and seaward side, having roughly 50% green vegetation would indicate a good recovery on the landward side of the shoreline; greater than 50% recovery indicates water pixels becoming vegetated.

Class	Barataria Bay		Chandeleur Islands		East Bird's Foot	
	2010	2011	2010	2011	2010	2011
Green Vegetation	199,985	278,078	9,724	20,455	29,351	31,015
NPV-Soil	69,191	14,763	9,071	10,672	913	208
Water	309,375	285,719	12,629	296	33,050	32,091
PCveg	34.6%	48.1%	30.9%	65.1%	46.4%	49.0%

There was a significant increase in green vegetation in 2011 at all three sites, although the degree of increase was site dependent (Table 4). In BB, vegetation increased by 13.5% (McNemar = 740.43 and a *p*-value < 0.0001). Of the area classified as NPV-Soil in 2010, 89.0% was revegetated in 2011, and 10.2% became water. Of the area classified as NPV-Soil in 2011, 90.8% had been previously classified as green vegetation in 2010. Thus, even though there was an overall increase in green vegetation, there was still turnover between the vegetation and NPV-soil classes. An important point to note is that in BB the NPV-Soil class only represented 12.0% of the classified area in 2010 and 5.2% in 2011.

In CI, the recovery was extensive; the area of green vegetation more than doubled from 2010 to 2011 (McNemar = 123.19, *p*-value < 0.0001). The area classified as NPV-Soil increased by 5.1%, with most of this change due to 2010 water pixels becoming NPV-Soil in 2011. The area classified as water decreased 98% from 2010 to 2011, with the majority pixels transitioning to green vegetation (Table 4). Much of this increase can be attributed to lower tide levels in the 2011 imagery, which made the vegetation easier to detect and explains why NPV-Soil replaced water. The green vegetation on these exposed sandbars may have been present in 2010, but because of the tides, it was not visible in the imagery.

We further investigated this "new" vegetation by comparing it to reference spectra of two dominant wetland species and performing a spectral mixture analysis to determine the proportion of soil and water in these pixels. The spectra of the "new" vegetation growth did not match the spectral signatures of either *S. alterniflora* or *A. germinans*. Our spectral mixture analysis found these pixels to be approximately 40% to 70% vegetation, with the rest being soil. These mixed vegetation-soil spectra made it impossible to identify the new vegetation at the species level.

In EBF, there was less change compared to the other two sites (McNemar = 19.81, *p*-value < 0.0001). Green vegetation increased by 2.6% from 2010 to 2011, and there was a steep decline in the area classified as NPV-Soil class, the majority of which was classified as green vegetation in 2011 (Table 4).

4. Discussion

The BP-DWH oil spill affected many sensitive ecosystems along the 1773 km of shoreline where oil was documented [33]. The AVIRIS data flown by NASA in response to this environmental disaster provided a rare opportunity to study the impact on these diverse ecosystems using hyperspectral imagery. Our study revealed the differential response of wetland plant communities to the apparently same level of oiling.

4.1. Comparison of Oil Impact across Sites

The tides do not inundate the entire upper marsh in BB except during the highest winter tides and in catastrophic events like hurricanes. BB's topography helped restrict oil pentration into the marsh to the highest tide level. Most of the oil was located within the first 3–4 pixels (10–15 m) from the shore which is mainly saltmarsh meadow dominated by two species, *S. alterniflora* and *J. roemerianus*. Both species are known for resilience to oil contamination [52–54], meaning that they recover from short-term exposures to oil, although long-term exposure may result in death [52]. DeLaune *et al*. [52] and Kirby and Grosselink [55], both showed that application of crude oil to *S. alterniflora* did not significantly impact plant biomass, stem density or new growth. However, when oil coats the leaf surface, productivity drops due to lack of gas exchange [53,54]. Similarly, for *J. roemerianus*, photosynthetic activity decreased when the plants were partially coated with oil and ceased when inundated completely. Photosynthetic activity started recovering after four weeks [54].

The first 7 m along the shore in BB were much more likely to contain vegetation with oil-covered stems and leaves, but further inland, the oil mainly coated the soil (Khanna, personal observation, September 2010). Additionally, Khanna *et al*. [13] showed that oil impact decreased the further the pixel was from the shore. To standardize our analysis across the three sites, we quantified oil impact in a single 16 m band along the shoreline. Thus, it is likely that the "small effect" in BB is due to the zone of severe impact being restricted to the first few meters adjacent to the shoreline and being combined with a much weaker impact further inland. Additionally, BB had the largest amount of shoreline for analysis of the three study sites. A larger shoreline for analysis is bound to encompass a greater range of impact, reducing the magnitude of the difference between the oiled and oil-free shorelines. Lastly, because of non-normal distributions for all the indices, we used a non-parametric test for significance. Non-parametric tests usually have less statistical power and thus can dampen differences between populations.

In CI, the dominant species were *A. germinans* and *S. alterniflora*, but their composition varied greatly across our study area. Some shorelines were co-dominated by *A. germinans* and *S. alterniflora* while other shorelines were mainly *S. alterniflora* interspersed with *A. germinans* (Figure 6). The resilience of *S. alterniflora* to oil contamination demonstrates a stark contrast to *A. germinans,* which, in general, is highly sensitive. Oil can disrupt ion transport in mangroves which is necessary for salt exclusion, an important mechanism for mangroves living in high salinity conditions. Other sub-lethal effects include branching of pneumatophores, decreased canopy cover, increased rate of mutation, inhibited respiration, and increased sensitivity to other stresses [56]. The mangroves grow in both high and low marshes in CI. The high marshes exist above the high, neap-tide line and are inundated only at especially high tides and storm surges, but the low marshes are inundated daily at high tide [57]. Thus mangroves can be impacted by oil irrespective of the distance from the shoreline if oil reaches their roots and pneumatophores. This is in contrast to BB where the oil injured or killed plants in the first few meters of the shoreline but had a weaker impact further inland.

Our analysis showed that EBF had the weakest impact of all three study sites. In EBF, the oiled sites were located in intermediate and freshwater marshes and were dominated almost entirely by *P. australis*. Previous reasearch has found that oiling of *P. australis* can decrease biomass, stem density, photosynthetic rates, and can cause the death of emerging buds, hindering reproduction [58–60]. However, Judy *et al*. [23] investigated the impact of the BP-DWH oil on *P. australis* in a greenhouse study. Their study found that applying the BP-DWH oil to the plant shoots had no significant negative impacts on plant growth and instead induced a vegetative stress response where *P. australis* produced side shoots. In contrast, when oil was applied directly to the soil, it produced a signicant reduction in plant growth. In the case of our study, field observations by Kokaly *et al*. [34] indicated that in EBF, oil came in with the water but did not settle on the soil. Kokaly *et al*. [34] further observed that the oil sometimes coated the leaves and stems of *P. australis* but did not damage the plant canopy. This differs from BB where the oil consistently covered the plants completely at the marsh edge forcing the vegetation to flatten under the weight of the oil [34]. We also hypothesize that because EBF continued

to receive fresh water from the Mississippi while the oil was coming ashore, it decreased or limited the residence time of the oil in the marsh.
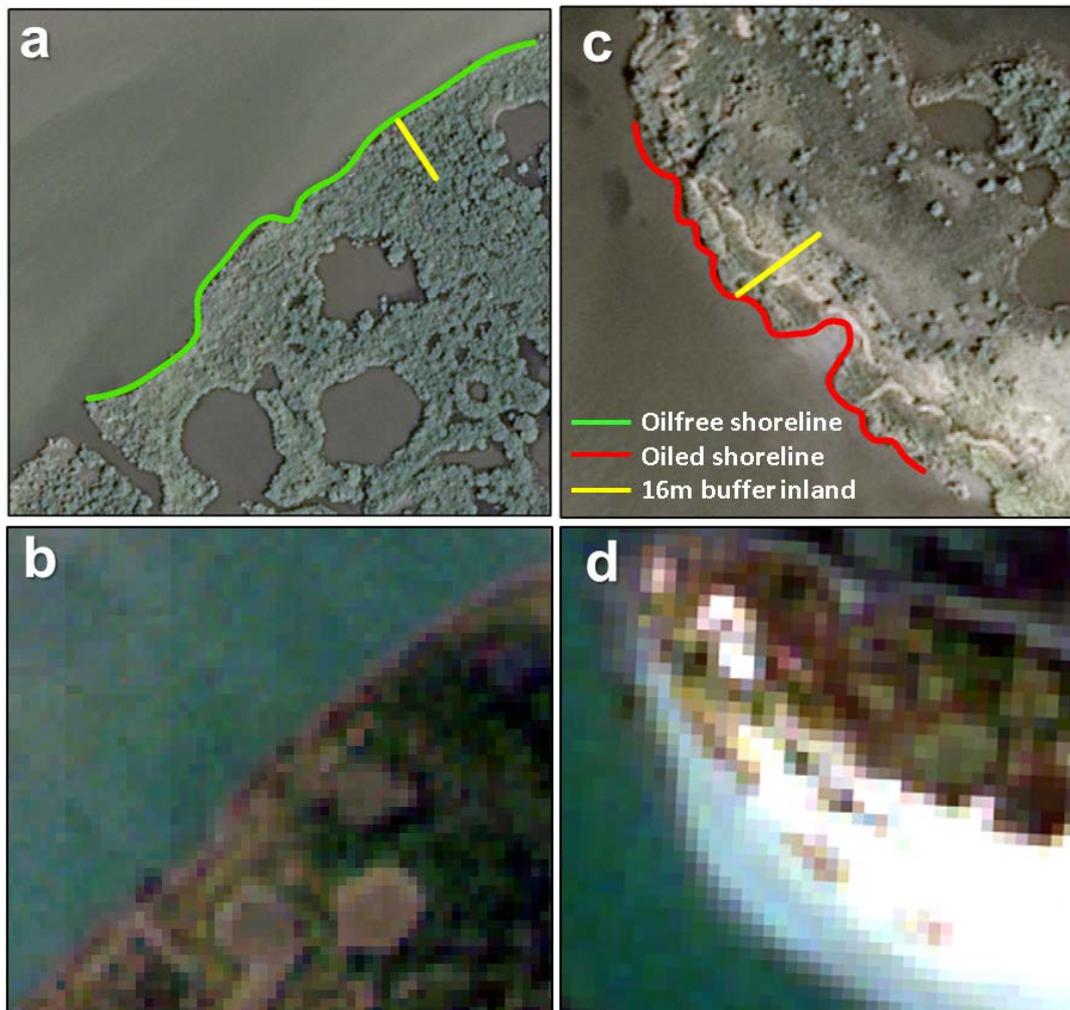

Figure 6. (**a**) SCAT shoreline data overlaid on 2010 GIS Aerometric 0.3 m imagery of a section of Chandeleur Islands with a yellow line marking the extent of the 16 meter buffer used in the analyses, (**b**) AVIRIS true color image showing the same extent of (**a**) at 7.7 m resolution, (**c**) SCAT shoreline data overlaid on 0.3m imagery of a section of Chandeleur Islands, (**d**) AVIRIS true color image showing the extent of (**c**) at 7.7 m resolution.

Our results indicate that CI was the most severely impacted of the three sites. However, CI also had the smallest subset of shoreline for analysis (Table 1). This means that the total length of shoreline affected in CI was small but the affected shore showed greater impact compared to the other two sites.

4.2. Comparison of Recovery from Oil across Sites

In BB, we saw a strong but incomplete recovery from 2010 to 2011. Several studies have shown that the dominant species in salt marshes are resilent to oiling in moderate to low doses and have good regrowth after canopy mortality under heavy oiling [7,24,53,61,62]. The lack of a full recovery in BB may be a consequence of looking at the mean response which is a combination of the strong impact that occurred in the first two pixels and the lower impact in the interior of the marsh.

CI exhibited the largest change of the three sites. Green vegetation more than doubled and a large majority of this newly vegetated area is a result of areas of water being converted to green vegetation.

Unlike the other two sites, these islands are constantly changing and being reshaped by wave action and as the underlying sand is reworked and deposited, new areas of land emerge as colonization sites [63]. Another contributing factor to the large change in green vegetation between years is the differing tide levels in the imagery (0.66 m in 2010 and 0.25 m in 2011). This tidal difference may explain some of the new vegetation found in 2011; however, the increase in green vegetation along oil-free shorelines was less than that along the oiled shorelines. Thus, tidal height difference does not explain all of the new vegetation in 2011.

The two dominant species on Chandeleur Islands, *S. alterniflora* and *A. germinans*, have different responses to oiling. Previous studies have shown that crude oil is highly detrimental to mangrove reproduction and easily kills mangrove seedlings [64]. Thus, one would not expect mangroves to show a strong recovery based on seedling establishment one year after oiling. As discussed in Section 3.2, spectral unmixing indicated a combination of soil plus vegetation, but the vegetation endmember signature could not be identified clearly. The tidal difference between the image dates may overestimate recovery, but new vegetation growth at CI is more likely from *S. alterniflora* rather than new mangroves.

In EBF, we saw a slight increase of green vegetation in 2011. This minimal response is consistent with the low impact observed in the vegetation indices. Having a constant supply of fresh water from the Mississippi River likely aided recovery in addition to lessening the original impact of oil by more rapid removal from the marsh.

5. Conclusions

The British Petroleum Deepwater Horizon oil spill affected a wide expanse of coastal ecosystems. Our examination of three ecologically diverse sites found different levels of vulnerability and resilience to oil. While Barataria Bay was the most extensively oiled site, it was more resilient to the deleterious effects of oil contamination compared to Chandeleur Islands which quantitatively had the least amount of heavily oiled shoreline. The impact on each site relied on the interplay between its topography, hydrology, and plant response. Hyperspectral imagery allowed us to track the changes in plant physiology across a spatially extensive area and over multiple years. This research has implications for future response to oil spills by highlighting the fact that areas subject to the most oil contamination may not be those most vulnerable to oil. Hence management decisions regarding clean-up and remediation need to take into account both the extent/severity of contamination and the sensitivity of ecosystems to that contamination. The Mississippi Deltaic Plain is still recovering from the effects of the 2010 oil spill and more studies are needed to look at long-term impacts across the many ecosystems that were affected. AVIRIS imagery has already been acquired over Barataria Bay in both 2012 and 2015 and analysis of this imagery currently underway will shed critical light on the long-term resilience of an ecosystem after an environmental disaster. Remotely sensed imagery is a powerful tool that can help cover the wide expanse of environmental disasters and document plant recovery in the following years.

Author Contributions: K. Shapiro researched, conceived, and performed the analysis, and wrote the paper. S. Khanna contributed to all aspects of the analysis, provided programming expertise, edited the paper, and advised on figure and table design. This research was conducted under the guidance of S. Ustin in her lab and she also contributed to the editing and organization of the paper.

Abbreviations

The following abbreviations are used in this manuscript:

ADW1	Absorption Depth of Water at 980 nm
ADW2	Absorption Depth of Water at 1240 nm
ANIR	Angle formed at NIR
ANOVA	ANalysis Of VAriance
ARed	Angle formed at Red
AVIRIS	Airborne Visible/Infrared Imaging Spectrometer
BB	Barataria Bay
BP-DWH	British Petroleum—DeepWater Horizon (oil spill)
CI	Chandeleur Islands
EBF	East Bird's Foot
ERMA	Environmental Response Management Application
MDP	Mississippi Deltaic Plain
mNDVI	modified Normalized Difference Vegetation Index
NASA	National Aeronautics and Space Administration
NDII	Normalized Difference Infrared Index
NDVI	Normalized Difference Vegetation Index
NIR	Near InfraRed
NOAA	National Oceanic and Atmospheric Administration
NPV	Non-photosynthetic vegetation
REIP	Red edge Inflexion Point
SCAT	Shoreline Cleanup Assessment Technique

References

1. Wiens, J.A. Review of an ecosystem services approach to assessing the impacts of the Deepwater Horizon Oil Spill in the Gulf of Mexico. *Fisheries* **2015**, *40*, 86–86. [CrossRef]

2. Ko, J.Y.; Day, J.W. A review of ecological impacts of oil and gas development on coastal ecosystems in the Mississippi Delta. *Ocean Coast. Manag.* **2004**, *47*, 597–623. [CrossRef]

3. Gosselink, J.G.; Pendleton, E.C. *The Ecology of Delta Marshes of Coastal Louisiana: A Community Profile*; U.S. Fish and Wildlife Service: Washington, D.C., USA, 1984; p. 156.

4. Couvillion, B.R.; Barras, J.A.; Steyer, G.D.; Sleavin, W.; Fischer, M.; Beck, H.; Trahan, N.; Griffin, B.; Heckman, D. *Land Area Change in Coastal Louisiana (1932 to 2010)*; USGS National Wetlands Research Center: Lafayette, LA, USA, 2011.

5. Silliman, B.R.; van de Koppel, J.; McCoy, M.W.; Diller, J.; Kasozi, G.N.; Earl, K.; Adams, P.N.; Zimmerman, A.R. Degradation and resilience in Louisiana salt marshes after the BP-Deepwater Horizon oil spill. *Proc. Natl. Acad. Sci. USA* **2012**, *109*, 11234–11239. [CrossRef] [PubMed]

6. Hester, M.W.; Mendelssohn, I.A. Long-term recovery of a Louisiana brackish marsh plant community from oil-spill impact: Vegetation response and mitigating effects of marsh surface elevation. *Mar. Environ. Res.* **2000**, *49*, 233–254. [CrossRef]

7. Pezeshki, S.R.; Hester, M.W.; Lin, Q.; Nyman, J.A. The effects of oil spill and clean-up on dominant US Gulf coast marsh macrophytes: A review. *Environ. Pollut.* **2000**, *108*, 129–139. [CrossRef]

8. Li, L.; Ustin, S.L.; Lay, M. Application of AVIRIS data in detection of oil-induced vegetation stress and cover change at Jornada, New Mexico. *Remote Sens. Environ.* **2005**, *94*, 1–16. [CrossRef]

9. Horler, D.N.H.; Dockray, M.; Barber, J. The red edge of plant leaf reflectance. *Int. J. Remote Sens.* **1983**, *4*, 273–288. [CrossRef]

10. Gitelson, A.; Merzlyak, M.N. Spectral reflectance changes associated with autumn senescence of *Aesculus hippocastanum* L. and *Acer platanoides* L. Leaves. Spectral features and relation to chlorophyll estimation. *J. Plant Physiol.* **1994**, *143*, 286–292. [CrossRef]

11. Tucker, C.J. Red and photographic infrared linear combinations for monitoring vegetation. *Remote Sens. Environ.* **1979**, *8*, 127–150. [CrossRef]

12. Hunt, E.R.; Rock, B.N. Detection of changes in leaf water content using near-infrared and middle-infrared reflectances. *Remote Sens. Environ.* **1989**, *30*, 43–54.

13. Khanna, S.; Santos, M.J.; Ustin, D.S.L.; Koltunov, A.; Kokaly, R.F.; Roberts, D.A. Detection of salt marsh vegetation stress after the Deepwater Horizon BP oil spill along the shoreline of gulf of Mexico using AVIRIS data. *PloS ONE* **2013**, *8*, e78989. [CrossRef] [PubMed]

14. Khanna, S.; Palacios-Orueta, A.; Whiting, M.L.; Ustin, S.L.; Riano, D.; Litago, J. Development of angle indexes for soil moisture estimation, dry matter detection and land-cover discrimination. *Remote Sens. Environ.* **2007**, *109*, 154–165. [CrossRef]

15. Dibner, P.C. *Response of A Salt Marsh to Oil Spill and Cleanup: Biotic and Erosional Effects in the Hackensack Meadowlands, New Jersey. Final report, May 1976–December 1977*; URS Research Co.: San Mateo, CA, USA, 1978.

16. Long, B.F.; Vandermeulen, J.H. Geomorphological impact of cleanup of an oiled salt marsh (Ile Grande, France). In Proceedings of the International Oil Spill Conference, San Antonio, Texas, USA, 28 February–3 March 1983; pp. 501–505.

17. Mishra, D.R.; Cho, H.J.; Ghosh, S.; Fox, A.; Downs, C.; Merani, P.B.T.; Kirui, P.; Jackson, N.; Mishra, S. Post-spill state of the marsh: Remote estimation of the ecological impact of the Gulf of Mexico oil spill on Louisiana Salt Marshes. *Remote Sens. Environ.* **2012**, *118*, 176–185. [CrossRef]

18. Rosso, P.H.; Pushnik, J.C.; Lay, M.; Ustin, S.L. Reflectance properties and physiological responses of *Salicornia virginica* to heavy metal and petroleum contamination. *Environ. Pollut.* **2005**, *137*, 241–252. [CrossRef] [PubMed]

19. Van der Meer, F.; van Dijk, P.; van der Werff, H.; Yang, H. Remote sensing and petroleum seepage: A review and case study. *Terra Nova* **2002**, *14*, 1–17. [CrossRef]

20. Yang, H.; Zhang, J.; van der Meer, F.; Kroonenberg, S.B. Geochemistry and field spectrometry for detecting hydrocarbon microseepage. *Terra Nova* **1998**, *10*, 231–235. [CrossRef]

21. Bammel, B.H.; Birnie, R.W. *Spectral Reflectance Response of Big Sagebrush to Hydrocarbon-Induced Stress in the Bighorn Basin, Wyoming*; American Society for Photogrammetry and Remote Sensing: Bethesda, MD, USA, 1994; Volume 60.

22. Khanna, S.; Santos, M.J.; Ustin, S.L.; Haverkamp, P.J. An integrated approach to a biophysiologically based classification of floating aquatic macrophytes. *Int. J. Remote Sens.* **2011**, *32*, 1067–1094. [CrossRef]

23. Judy, C.R.; Graham, S.A.; Lin, Q.; Hou, A.; Mendelssohn, I.A. Impacts of Macondo oil from Deepwater Horizon spill on the growth response of the common reed *Phragmites australis*: A mesocosm study. *Mar. Pollut. Bull.* **2014**, *79*, 69–76. [CrossRef] [PubMed]

24. Lin, Q.; Mendelssohn, I.A. Impacts and recovery of the Deepwater Horizon Oil Spill on vegetation structure and function of coastal salt marshes in the northern gulf of Mexico. *Environ. Sci. Technol.* **2012**, *46*, 3737–3743. [CrossRef] [PubMed]

25. Wu, W.; Biber, P.D.; Peterson, M.S.; Gong, C. Modeling photosynthesis of *Spartina alterniflora* (smooth cordgrass) impacted by the Deepwater Horizon oil spill using Bayesian inference. *Environ. Res. Lett.* **2012**, *7*, 045302. [CrossRef]

26. Visser, J.; Sasser, C.; Chabreck, R.; Linscombe, R.G. Marsh vegetation types of the Mississippi River Deltaic Plain. *Estuaries* **1998**, *21*, 818–828. [CrossRef]

27. Hymel, M. *Monitoring Plan for Chandeleur Islands Marsh Restoration*; LDNR/Coastal Restoration and Management: Baton Rouge, LA, USA, 2001; p. 12.

28. Day, J.; Britsch, L.; Hawes, S.; Shaffer, G.; Reed, D.; Cahoon, D. Pattern and process of land loss in the Mississippi Delta: A Spatial and temporal analysis of wetland habitat change. *Estuaries* **2000**, *23*, 425–438. [CrossRef]

29. Wilson, C.A.; Allison, M.A. An equilibrium profile model for retreating marsh shorelines in southeast Louisiana. *Estuar. Coast. Shelf Sci.* **2008**, *80*, 483–494. [CrossRef]

30. NOAA. Deepwater Horizon Data Integration Visualization Exploration and Reporting Application. Available online: http://dwhdiver.orr.noaa.gov (accessed on 31 January 2016).

31. CWPPRA. The Mississippi River Delta Basin. Available online: http://lacoast.gov/new/About/Basin_data/mr/ (accessed on 31 January 2016).

32. USGS. Coastwide Reference Monitoring System. Available online: http://lacoast.gov/crms2/ (accessed on 31 January 2016).

33. Michel, J.; Owens, E.H.; Zengel, S.; Graham, A.; Nixon, Z.; Allard, T.; Holton, W.; Reimer, P.D.; Lamarche, A.; White, M.; *et al.* Extent and degree of shoreline oiling: *Deepwater Horizon* oil spill, Gulf of Mexico, USA. *PLoS ONE* **2013**, *8*, e65087. [CrossRef] [PubMed]

34. Kokaly, R.F.; Heckman, D.; Holloway, J.; Piazza, S.C.; Couvillion, B.R.; Steyer, G.D.; Mills, C.T.; Hoefen, T.M. *Shoreline Surveys of Oil-Impacted Marsh in Southern Louisiana, July to August 2010: Open-File Report 2011-1022*; USGS Crustal Geophysics and Geochemistry Science Center: Denver, CO, USA, 2011.

35. Cretini, K.F.; Visser, J.M.; Krauss, K.W.; Steyer, G.D. *CRMS Vegetation Analytical Team Framework: Methods for Collection, Development, and Use of Vegetation Response Variables*; USGS National Wetlands Research Center: Lafayette, LA, USA, 2011; p. 60.

36. Palacios-Orueta, A.; Khanna, S.; Litago, J.; Whiting, M.L.; Ustin, S.L. Assessment of NDVI and NDWI spectral indices using MODIS time series analysis and development of a new spectral index based on MODIS shortwave infrared bands. In Proceedings of the 1st International Conference of Remote Sensing and Geoinformation Processing, Trier, Germany, 7–9 September 2005.

37. Friedl, M.A.; Brodley, C.E. Decision tree classification of land cover from remotely sensed data. *Remote Sens. Environ.* **1997**, *61*, 399–409. [CrossRef]

38. Hickman, J.C. *The Jepson Manual: Higher Plants of California*; University of California Press: Berkeley, CA, USA, 1993.

39. Biello, M.; Rust, D.; Watkins, T. Oil laps barrier islands; BP grilled about oil spill at Capitol. Available online: http://www.cnn.com (accessed on 4 May 2010).

40. Guillot, C. Oil spill hits gulf coast habitats. Available online: http://news.nationalgeographic.com (accessed on 30 April 2010).

41. Strassmann, M. The fight over keeping oil out of Barataria Bay. Available online: http://www.cbsnews.com (accessed on 7 July 2010).

42. Ustin, S.L.; Roberts, D.A.; Khanna, S.; Shapiro, K.; Beland, M.; Peterson, S.; Roth, K. *Coastal Wetland and Near Shore Ecosystem Impacts from the Gulf of Mexico Deepwater Horizon BP Oil Spill Monitored by NASA's AVIRIS and MASTER Imagers*; NASA: Davis, CA, USA, 2014.

43. Kokaly, R.F.; Couvillion, B.R.; Holloway, J.M.; Roberts, D.A.; Ustin, S.L.; Peterson, S.H.; Khanna, S.; Piazza, S.C. Spectroscopic remote sensing of the distribution and persistence of oil from the Deepwater Horizon spill in Barataria Bay marshes. *Remote Sens. Environ.* **2013**, *129*, 210–230. [CrossRef]

44. Peterson, S.H.; Roberts, D.A.; Beland, M.; Kokaly, R.F.; Ustin, S.L. Oil detection in the coastal marshes of Louisiana using MESMA applied to band subsets of AVIRIS data. *Remote Sens. Environ.* **2015**, *159*, 222–231. [CrossRef]

45. Mann, H.B.; Whitney, D.R. On a test of whether one of two random variables is stochastically larger than the other. *Ann. Math. Stat.* **1947**, *18*, 50–60. [CrossRef]

46. Macbeth, G.; Razumiejczyk, E.; Ledesma, R.D. Cliff's Delta Calculator: A non-parametric effect size program for two groups of observations. *Univ. Psychol.* **2011**, *10*, 545–555.

47. Cliff, N. Dominance statistics: Ordinal analyses to answer ordinal questions. *Psychol. Bull.* **1993**, *114*, 494–509. [CrossRef]

48. Romano, J.; Kromrey, J.D.; Coraggio, J.; Skowronek, J.; Devine, L. Exploring methods for evaluating group differences on the NSSE and other surveys: Are the t-test and Cohen's d indices the most appropriate choices? In Proceedings of the Annual Meeting of the Southern Association for Institutional Research, Arlington, VA, USA, 14–17 October 2006.

49. Dai, X.L.; Khorram, S. The effects of image misregistration on the accuracy of remotely sensed change detection. *ITGRS* **1998**, *36*, 1566–1577.

50. Khorram, S.; Biging, G.S.; Chrisman, N.R.; Colby, D.R.; Congalton, R.G.; Dobson, J.E.; Ferguson, R.L.; Goodchild, M.R.; Jensen, J.R.; Mace, T.H. *Accuracy Assessment of Remote Sensing Derived Change Detection*; American Society of Photogrammetry and Remote Sensing (ASPRS): Bethesda, MD, USA, 1998.

51. McNemar, Q. Note on the sampling error of the difference between correlated proportions or percentages. *Psychometrika* **1947**, *12*, 153–157. [CrossRef] [PubMed]

52. DeLaune, R.D.; Patrick, W.H., Jr.; Buresh, R.J. Effect of crude oil on a Louisiana *Spartina alterniflora* salt marsh. *Environ. Pollut.* **1979**, *20*, 21–31. [CrossRef]

53. DeLaune, R.D.; Pezeshki, S.R.; Jugsujinda, A.; Lindau, C.W. Sensitivity of US Gulf of Mexico coastal marsh vegetation to crude oil: Comparison of greenhouse and field responses. *Aquat. Ecol.* **2003**, *37*, 351–360. [CrossRef]

54. Pezeshki, S.R.; DeLaune, R.D. Effect of crude oil on gas exchange functions of *Juncus roemerianus* and *Spartina alterniflora*. *Water Air Soil Pollut.* **1993**, *68*, 461–468. [CrossRef]

55. Kirby, C.J.; Gosselink, J.G. Primary Production in a Louisiana Gulf Coast *Spartina Alterniflora* Marsh. *Ecology* **1976**, *57*, 1052–1059. [CrossRef]

56. Hoff, R.; Hensel, P.; Proffitt, E.C.; Delgado, P.; Shigenaka, G.; Yender, R.; Mearns, A.J. *Oil Spills in Mangroves: Planning & Response Considerations*; U.S. Department of Commerce, NOAA: Seattle, WA, USA, 2010; p. 72.

57. Hester, M.W.; Spalding, E.A.; Franze, C.D. Biological resources of the Louisiana Coast: Part 1. An overview of coastal plant communities of the Louisiana gulf shoreline. *J. Coast. Res.* **2005**, 134–145. Available online: http://www.jstor.org/stable/25737053 (accessed on 22 April 2016).

58. Dowty, R.A.; Shaffer, G.P.; Hester, M.W.; Childers, G.W.; Campo, F.M.; Greene, M.C. Phytoremediation of small-scale oil spills in fresh marsh environments: A mesocosm simulation. *Mar. Environ. Res.* **2001**, *52*, 195–211. [CrossRef]

59. Lin, Q.; Mendelssohn, I.A.; Hester, M.W.; Webb, E.C.; Henry, J.; Charles, B. Effect of oil cleanup methods on ecological recovery and oil degradation of *Phragmites* marshes. *Int. Oil Spill Conf. Proc.* **1999**, *1999*, 511–517. [CrossRef]

60. Armstrong, J.; Keep, R.; Armstrong, W. Effects of oil on internal gas transport, radial oxygen loss, gas films and bud growth in *Phragmites australis*. *Ann. Bot.* **2009**, *103*, 333–340. [CrossRef]

61. DeLaune, R.D.; Wright, A.L. Projected impact of Deepwater Horizon oil spill on U.S. gulf coast wetlands. *Soil Sci. Soc. Am. J.* **2011**, *75*, 1602–1612. [CrossRef]

62. Smith, C.J.; Delaune, R.D.; Patrick, W.H.; Fleeger, J.W. Impact of dispersed and undispersed oil entering a gulf coast salt marsh. *Environ. Toxicol. Chem.* **1984**, *3*, 609–616. [CrossRef]

63. Hayden, B.P.; Santos, M.C.F.V.; Shao, G.; Kochel, R.C. Geomorphological controls on coastal vegetation at the Virginia Coast Reserve. *Geomo* **1995**, *13*, 283–300. [CrossRef]

64. Grant, D.L.; Clarke, P.J.; Allaway, W.G. The response of grey mangrove (*Avicennia marina* (Forsk.) Vierh.) seedlings to spills of crude oil. *J. Exp. Mar. Biol. Ecol.* **1993**, *171*, 273–295. [CrossRef]